weighing 5 to 20 mg from the 60- to 100-mesh fraction. Whole-rock samples were of matrix (phenocrysts removed) material crushed to 20- to 40-mesh size. The first analysis of each sample (46-WR.A and 2-WR.A) was on single grains of this material, the second was each on four grains. All samples (plagioclase and whole rock) were rinsed in dilute HCl and HF.

19. The effects of ^{39}Ar recoil loss and redistribution on apparent age spectra are discussed by G. Turner and P. H. Cadogan, *Geochim. Cosmochim. Acta Suppl. 5* **2**, 1601 (1974); J. C. Huneke, *Earth Planet. Sci. Lett.* **28**, 407 (1976); G. A. Schaeffer and O. A. Schaeffer, *Proc. Lunar. Sci. Conf.* **8**, 2253 (1977).
20. G. T. Cebula *et al.*, *TERRA Cognita* **6**, 139 (1986). The age of 27.84 Ma for Fish Canyon sanidine is consistent with an age of 520.4 Ma given by S. D. Samson and E. C. Alexander [*Chem. Geol. Isot. Geosci. Sect.* **66**, 27 (1987)] for the interlaboratory standard Mmhb-1. The corresponding *J*-value calculated from individual laser fusion of seven grains is $1.9104 \times 10^{-2} \pm 1.6978 \times 10^{-5}$.
21. Samples were incrementally heated by stepwise increasing power output from an Ar-ion laser with defocused beam. Laser power output, pneumatically actuated valve operation, and mass spectrometer operation (magnetic field jumping and detector output reading) were automated using procedures described by A. L. Deino and R. Potts [*J. Geophys. Res.* **95**, 8453 (1990)], A. Deino, L. Tauxe, M. Monaghan, and R. Drake [*J. Geol.* **98**, 567 (1990)], P. R. Renne, T. A. Becker, and S. M. Swapp [*Geology* **18**, 563 (1990)], P. R. Renne, M. M. Fulford, and C. J. Busby-Spera [*Geophys. Res. Lett.* **18**, 459 (1991)], and C. C. Swisher and D. R. Prothero [*Science* **249**, 760 (1990)]. A cryocooled cold-trap on the extraction line was operated at −50°C to help remove condensable gases. Uncertainties in dates are reported at the 2σ level and include contributions from uncertainties in isotope ratio regressions, corrections for mass discrimination, atmospheric contamination and interfering nucleogenic isotopes, and uncertainty in the $^{40}Ar^*/^{39}Ar_K$ of the standards, but do not include uncertainty in the age of the standard. Mass discrimination (1.0069 ± 0.0020 per atomic mass unit) was monitered by automated analysis of 20 air pipette samples interspersed with the sample analyses.
22. We define a plateau as comprising three or more contiguous steps with apparent ages that overlap the mean at the 2σ level excluding error contribution from the *J*-value. This definition is similar to that employed by R. J. Fleck *et al.* [*Geochim. Cosmochim. Acta* **41**, 15 (1977)] except that we do not stipulate that a plateau must contain any specific minimum proportion of the total Ar released. Our plateau dates are calculated as the weighted (by inverse variances) mean of all steps defining a plateau. Because errors in individual step dates are largely an inverse function of the Ar volume analyzed, the inverse variance weighting scheme produces results similar to schemes based on relative ^{39}Ar abundance.
23. Regression of $^{36}Ar/^{40}Ar$ versus $^{39}Ar/^{40Ar}$ followed the technique of D. York [*Earth Planet. Sci. Lett.* **5**, 320 (1969)] and yielded the following results: For 46-WR, date = 248.2 ± 1.2 Ma, $(^{40}Ar/^{36}Ar)_0$ = 287.6 ± 31.0, N = 15, MSWD = 0.475; for 46-PL, date = 249.5 ± 1.2 Ma, $(^{40}Ar/^{36}Ar)_0$ = 259.5 ± 26.3, N = 9, MSWD = 0.722; for 42-PL, date = 246.4 ± 2.2 Ma, $(^{40}Ar/^{36}Ar)_0$ = 292.0 ± 23.4, N = 10, MSWD = 1.052; for 2-WR, date = 246.3 ± 4.3 Ma, $(^{40}Ar/^{36}Ar)_0$ = 315.0 ± 41.2, N = 8, MSWD = 1.860.
24. The volume estimate is based on the proportion of maximum composite stratigraphic thickness represented by flows older than the Kharaelakhsky suite (Fig. 2), and the assumption that there is a consistent relation between thickness and volume.
25. R. A. Duncan and M. A. Richards, *Rev. Geophys.* **29**, 31 (1991).
26. G. F. Marenko, *Int. Geol. Rev.* **19**, 1089 (1976).
27. The dates are based on an age of 27.84 Ma for Fish Canyon sanidine (*20*). Recent studies by M. A. Lanphere *et al.* [*Proceedings of the Seventh International Conference on Geochronology, Cosmochronology, and Isotope Geology* (Abst.), Canberra (1990), p. 57] and C. C. Swisher (*ibid.*, p. 98) indicate that this age may be in error by as much as 1%. Recalculating uncertainty in the neutron fluence parameter *J* with a 1% uncertainty in age (at the 95% confidence level) yields a value of $2\sigma_J = 1.9326 \times 10^{-4}$. With the pooled mean plateau value of $^{40}Ar^*/^{39}Ar_K = 7.7256 \pm 0.0099$ for sample 46, a date of 248.4 ± 2.4 Ma (2σ) is obtained that reflects uncertainty in the age of the standard and is appropriate for external comparison.
28. R. L. Armstrong, in *Contributions to the Geologic Time Scale*, G. V. Cohee, M. F. Glaessner, H. D. Hedberg, Eds. (*Stud. Geol. 6*, American Association of Petroleum Geologists, Tulsa, 1978), pp. 73–91; K. N. Hellman and H. J. Lippolt, *J. Geophys.* **50**, 73 (1981); J. A. Webb, *J. Geol. Soc. Austral.* **28**, 107 (1981); G. S. Odin and W. J. Kennedy, *C. R. Seances Acad. Sci. Paris* **294**, 453 (1982); W. B. Harland *et al.*, *A Geologic Time Scale* (Cambridge Univ. Press, Cambridge, 1982); A. R. Palmer, *Geology* **11**, 503 (1983); S. C. Forster and G. Warrington, in *The Chronology of the Geological Record*, N. J. Snelling, Ed. (Blackwell, Palo Alto, 1985), pp. 99–113; G. S. Odin, in *ibid*, pp. 114–117.
29. N. D. Newell, in *The Permian and Triassic Systems and Their Mutual Boundary*, A. Logan and L. V. Hills, Eds. (*Mem. 2*, Canadian Society of Petroleum Geologists, Calgary, 1973), pp. 1–10.
30. This research was supported by the Institute of Human Origins and National Science Foundation grant EAR 8805781. We are indebted to G. V. Nesterenko for providing samples and geologic context; T. A. Becker for assistance in the Ar laboratory; D. Beckner for graphics; W. Alvarez, G. H. Curtis, G. Czamanske, D. J. DePaolo, R. A. Duncan, and M. Sharma for discussions; M. A. Richards, C. C. Swisher, and R. C. Walter, plus three anonymous reviewers, for constructive criticism of the manuscript.

11 March 1991; accepted 15 May 1991

Solution Structures of β Peptide and Its Constituent Fragments: Relation to Amyloid Deposition

COLIN J. BARROW* AND MICHAEL G. ZAGORSKI†

The secondary structures in solution of the synthetic, naturally occurring, amyloid β peptides, residues 1 to 42 [β(1-42)] and β(1-39), and related fragments, β(1-28) and β(29-42), have been studied by circular dichroism and two-dimensional nuclear magnetic resonance spectroscopy. In patients with Alzheimer's disease, extracellular amyloid plaque core is primarily composed of β(1-42), whereas cerebrovascular amyloid contains the more soluble β(1-39). In aqueous trifluoroethanol solution, the β(1-28), β(1-39), and β(1-42) peptides adopt monomeric α-helical structures at both low and high pH, whereas at intermediate pH (4 to 7) an oligomeric β structure (the probable structure in plaques) predominates. Thus, β peptide is not by itself an insoluble protein (as originally thought), and localized or normal age-related alterations of pH may be necessary for the self-assembly and deposition of β peptide. The hydrophobic carboxyl-terminal segment, β(29-42), exists exclusively as an oligomeric β sheet in solution, regardless of differences in solvent, pH, or temperature, suggesting that this segment directs the folding of the complete β(1-42) peptide to produce the β-pleated sheet found in amyloid plaques.

ALZHEIMER'S DISEASE (AD) IS characterized by extracellular deposits in the form of amyloid plaques (*1*). The major protein constituent of plaques is β peptide (Fig. 1), which is a small (39 to 43 amino acids) polypeptide (*2, 3*) derived from a larger (695, 714, 751, or 770 amino acids) amyloid precursor protein (APP) (*4*). The majority of recent research into AD has focused on APP; that is, investigations have focused on the relations of different APP forms to AD (*5*) and the normal and alternative pathways by which APP molecules can be proteolytically processed (*6*). However, less information is known about the amyloid β peptide than about APP, especially on a molecular level (*7, 8*), because β peptide is extremely insoluble and has a high propensity to aggregate. This latter property is presumably related to its tendency to produce oligomeric β structures, the probable conformation in plaques (*9, 10*).

The circular dichroism (CD) spectra for freshly prepared solutions of β peptide and some fragments, in aqueous 5 mM phosphate buffer at pH 7.3 and 22.0°C, are shown in Fig. 2A. Analysis of these spectra by the method of Greenfield and Fasman (*11*), together with computer fitting (*12*) to polylysine standard curves, gives approximately 90 and 100% β-sheet structure for the β(1-42) and β(29-42) peptides, respectively. In contrast, the β(1-28) peptide is essentially random coil, and the β(1-39) peptide is a mixture of random coil and β-sheet structures in an approximate ratio of

Suntory Institute for Bioorganic Research, Wakayamadai, Shimamoto-cho, Mishima-gun, Osaka 618, Japan.

†To whom correspondence should be addressed.
*Present address: Sterling Drug, 9 Great Valley Parkway, Malvern, PA 19355.

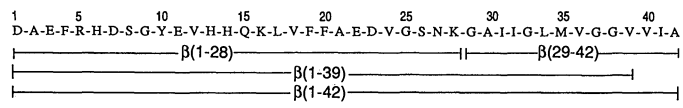

Fig. 1. Sequences of the four β peptides investigated in this study (*25*). The parent β peptide [β(1-42)] found in amyloid plaques generally consists of 42 residues (*2, 3*). Peptides were synthesized by solid-phase methods on an automated (Applied Biosystems 430A) synthesizer with the use of standard methodology (*26*). The crude peptides were deprotected in anhydrous HF and then purified by trituration in ether and reverse-phase high-performance liquid chromatography with C_4 columns (Cosmasil $5C_4$-300 and Vydac 214TP510). Peptide identity was verified by amino acid analysis and mass spectroscopy.

1:1. In solutions containing up to 50% trifluoroethanol (TFE), which promotes intramolecular hydrogen bonding (*13*), the β(29-42) peptide remains in a β-sheet conformation. However, TFE stabilizes the formation of α-helical structures in the β(1-28), β(1-39), and β(1-42) peptides, indicating that the hydrophilic NH_2-terminal region of β peptide can form random coil, β-sheet or α-helical structures depending on external solution conditions. Under equivalent conditions, an α-helical structure is more easily formed in β(1-39) than in β(1-42), indicating that β(1-42) forms a more stable β-sheet structure than does β(1-39) (Fig. 2, B and C). The secondary structure of β(1-39) in aqueous solution containing TFE is similar to that of β(1-28), although for β(1-42) the COOH-terminal amino acids appear to encourage β-sheet formation.

The CD spectra for β(1-39) and β(1-42) in Fig. 2 were taken 20 min after dissolution. When CD spectra were remeasured consecutively at 20-min intervals, the curves for both low and high pH solutions remained essentially unchanged, whereas for solutions at pH 4 to 7 there was a progressive change in the CD curve corresponding to complete β-sheet formation and then a shift in the single minimum at 217 nm to higher wavelength and lower intensity, until finally only baseline spectra were observed. Centrifugation at this point revealed the presence of solid material consistent with the formation of plaque-like aggregates. The most rapid rate of aggregation occurred at approximately pH 5.5, and aggregation was more rapid for β(1-42) than for β(1-39). Aqueous solutions of β(1-42), in the absence of TFE, at either low or high pH gave CD curves with one minimum at 217 nm, which is consistent with 100% β sheet. These results indicate that a decrease in pH from 7.3 (blood pH) causes an increase in the rate of aggregation of β peptide, with a maximum occurring at approximately pH 5.5.

The amount of β-sheet structure formed by β(29-42) was concentration-dependent over the range from 0.03 to 3.0 mM, and alterations of temperature or pH did not show any observable changes by CD. In contrast, for β(1-28) at pH 2.8 and 7.4, we observed no concentration dependence for the α-helical structure, indicating that helix formation is monomeric. However, β(1-28) can form a plaque-like intermolecular β-sheet structure (*10*). The conformational behavior of this region of β peptide is complex, with ratios of β structure, α helix, and random coil being strongly dependent on solution conditions. To understand the contribution of this region to plaque formation, we further investigated the solution behavior of the β(1-28) peptide by nuclear magnetic resonance (NMR) spectroscopy.

The solution behavior of β(1-28) is similar to that of β(1-39) and β(1-42) in that the α helix is destabilized at pH 4 to 7 and at increased temperature. The β sheet is formed preferentially to the α-helical structure in this midrange pH region for these peptides. We used a more concentrated sample (3.5 mM) of β(1-28) for the NMR spectroscopic work than for the CD studies. For this 3.5-mM solution, when the pH was raised from 3.0 to 4.5 or decreased from 7.3 to 6.8, the solution immediately turned into a gel that could only be dissolved in concentrated acid. This result demonstrates that the β-sheet structure observed at pH 4 to 7 is intermolecular. Similar behavior was reported for β peptide isolated from plaques (*3*), where it was determined by gel permeation chromatography that monomeric forms exist at low pH. All of the proton NMR spectra were obtained with a 6-mg (3.5-mM) sample of β(1-28) prepared in a TFE-d_2:H_2O (6:4) buffered solution at 25.0°C and pH 3.0. A one-dimensional (1D) spectrum obtained at a protein concentration of 0.35 mM was virtually identical to that obtained at 3.5 mM. Therefore, as previously shown by CD, at pH 3.0 it appears that no further aggregation occurs with increasing concentration. If β(1-28) were associating at higher concentrations, large changes in both the line widths and chemical shifts of the amide resonances should be observed (*14*).

The complete proton NMR spectrum was assigned with the use of standard methodology (*15*). Figure 3 shows an expanded region of a 2D nuclear Overhauser enhancement spectroscopy (NOESY) spectrum where cross-peaks correspond to through-space interactions [nuclear Overhauser effects (NOEs)] among the amides (NHs) of neighboring amino acid residues. A complete listing of the interresidue NOEs is shown in Fig. 4; the NOEs between neighboring amides are listed as NN(i, i + 1). These latter NOEs, together with the weaker intensity αN(i, i + 1) and medium intensity αN(i, i + 2), αN(i, i + 3), and αβ(i, i +

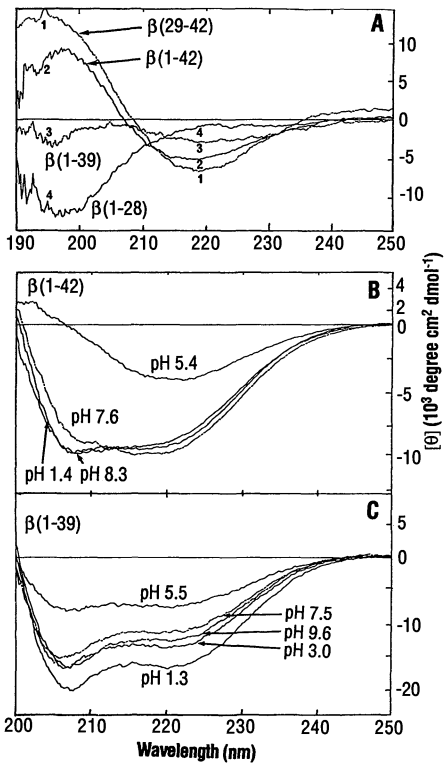

Fig. 2. The CD spectra of amyloid β peptides taken at 22.0°C in buffered water (5 mM potassium phosphate) or buffered water plus TFE solutions. Peptides β(1-42) and β(29-42) are sparingly soluble in aqueous solution. Therefore, to overcome problems related to the insolubility of the peptides in aqueous solution, we prepared stock solutions in hexafluoro-2-propanol, removed aliquots from these stock solutions, and diluted these aliquots 1000-fold in the buffered water or buffered water plus TFE solutions used for CD analysis. Spectra were taken on a Jasco spectropolarimeter (model J-600) 20 min after peptide dissolution and are reported in units of mean residue ellipticity (degrees cm^2 $dmol^{-1}$). Data were taken with a 0.2-nm step size and a 1-s average time and were averaged over four scans. (**A**) β(29-42) (curve 1), β(1-42) (curve 2), β(1-39) (curve 3), and β(1-28) (curve 4) peptides in water, pH 7.3. Peptide concentrations were 15 μM. (**B**) β(1-42) in TFE:H_2O (1:3) at pH values, as indicated. Peptide concentration was 15 μM. Data obtained at pH 3.0 and 9.6 were identical to the data shown at pH 1.4 and 8.3, respectively. (**C**) β(1-39) in TFE:H_2O (1:3) at different pH values, as indicated. Peptide concentration was 5 μM. Variations of CD spectra with pH for β(1-28) were similar to those observed for β(1-39), whereas data for β(29-42) were insensitive to pH.

3) NOEs, indicate that a helical segment is present from Tyr^{10} or Glu^{11} to Ser^{26}. The presence of $\alpha N(i, i + 4)$ NOEs rules out the possibility of a 3_{10} helix. Another less stable and shorter helix is present at the NH_2 terminus within the Ala^2 to His^6 stretch, as indicated with medium intensity $NN(i, i + 1)$ NOEs and weaker intensity $\alpha N(i, i + 1)$ NOEs but the lack of additional $\alpha N(i, i + 3)$ and $\alpha\beta(i, i + 3)$ NOEs suggests a mixture of extended chain and helical conformations. Predictions (*10*) indicate that the Asp^7 to Tyr^{10} segment, which connects the two helices, probably exists in a reverse turn, given the presence of the polar Ser^8 at position $i + 1$ [Ser is the amino acid most frequently found in reverse turns (*16*)] and Gly^9 at position $i + 2$ (*17*). However, if a reverse turn is present, additional NOE and coupling constant data are needed to more clearly define its exact type.

The ability of β peptide to exist either in a monomeric α-helical or an oligomeric β-sheet conformation may be relevant in vivo to the production of plaques in AD. Indeed, β peptide is known to exist in distinct states of aggregation in different lesions (*18*). One possibility is that, in normal individuals, β peptides in blood (*19*) and other "preamyloid" deposits (*20*), which may naturally occur as normal proteolytic processing products of APP, are soluble and do not precipitate as plaques rapidly enough to avoid breakdown by further proteolysis. However, in normal, aged individuals and AD patients, localized changes in pH or temperature or inclusion of nonproteinaceous materials such as aluminum, silicon, and carbohydrates [components colocalized in the central region of senile plaques (*21*)] may speed up plaque formation so that proteolysis of β peptide is no longer possible. The sensitivity of β peptide conformation to pH is especially significant because in degenerating neurons, typically found in AD patients, a lack of oxygen can cause localized alterations of pH (*22*). Thus perhaps a decrease in the supply of oxygen, changes in localized neurotransmitter concentrations, or degenerating neurons, which are known to alter extracellular pH by releasing lysosomes and other cathepsin-laden vesicles (*23*), are responsible for the changes in pH that may cause β peptide to deposit as plaques (*24*).

In addition, at pH 4 to 7 the β(1-42) peptide forms an aggregated β-sheet structure faster than the β(1-39) peptide, suggesting that the Val^{40} to Ala^{42} segment is critical for stabilization in solution of the β sheet, which is probably the structure formed before formation of the β-pleated sheet structure of the amyloid plaques. Recent work by Halverson and co-workers (*8*) also supports this view because β(34-42), but not β(29-33), adopts an antiparallel β-sheet structure in the solid state. Thus, perhaps the less soluble β(1-42) peptide, which is the predominant form in plaques and fibrils, is the product from a defective proteolysis of APP that may occur during AD, whereas the β(1-39) peptide, found predominantly in blood, is the product from a normal proteolysis of APP.

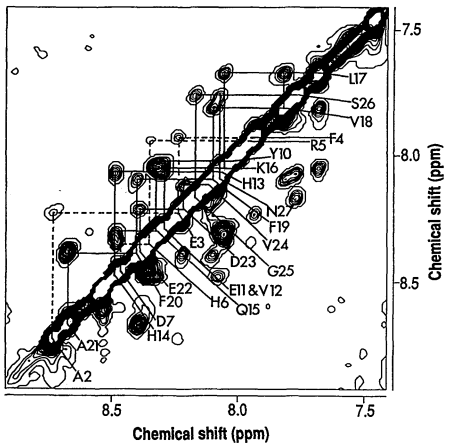

Fig. 3. Expanded phase-sensitive NOESY (1024 by 1024 points) contour plot of the NH-NH region. Spectra were recorded at 500 MHz on a GN-500 spectrometer from a 3.5-mM sample of β(1-28) in buffered (5 mM potassium phosphate) $CF_3CD_2OD:H_2O$ (6:4) solution at pH 3.0 and 25.0°C. The data were acquired with the following parameters: spectral widths of ±2500 Hz, 2048 points in the t_2 dimension and 256 complex points in the t_1 dimension, recycle delay 2s, mixing time 150 ms. H_2O was suppressed by presaturation. Data were processed on a Sun 3/60 computer with the use of NMR2 software (New Methods Research, Syracuse, New York) with minor modifications. Assignments of NHs are shown along the diagonal. Cross-peaks are diagnostic for $NN(i, i + 1)$ NOEs, or interactions between protons close in space (2.4 to 3.6 Å) (*15*). Connections between NHs of residues within the Ala^2 to Asp^6 and Tyr^{10} to Ser^{26} segments are shown with dotted and solid lines, respectively.

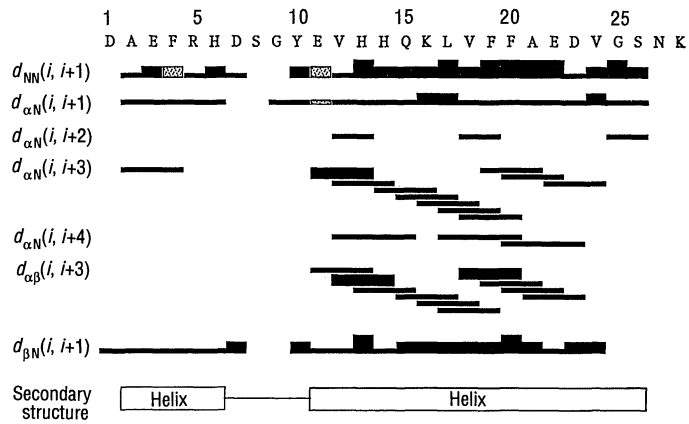

Fig. 4. A summary of the sequential NOEs involving NH, αCH, and βCH protons for β(1-28). Only interresidue NOEs are shown; that is, $d\alpha N(i, i + 1)$ corresponds to an observed NOE between the αCH proton of residue i with the NH proton of residue $i + 1$ (*15*). The intensities of the NOEs are classified according to the thickness of the bar heights. Where unambiguous assignment was not possible because of peak overlap, NOE connections are drawn with dotted boxes. Appropriate corrections for the intensities of NOEs among the exchangeable NHs were made because the solvent mixture (60% CF_3CD_2OD and 40% H_2O) contains 43% exchangeable deuterium. The secondary structures deduced from the NOE data are shown at the bottom.

REFERENCES AND NOTES

1. H. M. Wisniewski, H. K. Narang, R. Terry, *J. Neurol. Sci.* **27**, 173 (1976); D. L. Price, *Annu. Rev. Neurosci.* **9**, 489 (1986); K. Beyreuther *et al.*, in *Etiology of Dementia of Alzheimer's Type*, A. S. Henderson and J. H. Henderson, Eds. (Wiley, New York, 1988), pp. 125–134; G. G. Glenner, *Cell* **52**, 307 (1988); B. Muller-Hill and K. Beyreuther, *Annu. Rev. Biochem.* **58**, 287 (1989); D. J. Selkoe, *Annu. Rev. Neurosci.* **12**, 463 (1989).
2. G. G. Glenner and C. W. Wong, *Biochem. Biophys. Res. Commun.* **120**, 885 (1984); D. J. Selkoe, C. R. Abraham, M. B. Podlisny, L. K. Duffy, *J. Neurochem.* **46**, 1820 (1986).
3. C. L. Masters *et al.*, *Proc. Natl. Acad. Sci. U.S.A.* **82**, 4245 (1985).
4. J. Kang *et al.*, *Nature* **325**, 733 (1987); D. Goldgaber, M. I. Lerman, O. W. McBride, U. Saffiotti, D. C. Gajdusek, *Science* **235**, 877 (1987); R. E. Tanzi *et al.*, *Nature* **331**, 528 (1988); N. Kitaguchi, Y. Takahashi, Y. Tokushima, S. Shiojiri, H. Itoh, *ibid.* p. 530; F. de Sauvage and J.-N. Octave, *Science* **245**, 651 (1989); T. Oltersdorf *et al.*, *J. Biol. Chem.* **265**, 4492 (1990).
5. M. R. Palmerf *et al.*, *Science* **241**, 1080 (1988); S. A. Johnson, T. McNeill, B. Cordell, C. E. Finch, *ibid.* **248**, 854 (1990).
6. A. Weidemann *et al.*, *Cell* **57**, 115 (1989); M. R. Palmert *et al.*, *Proc. Natl. Acad. Sci. U.S.A.* **86**, 6338 (1989); H. Zhang *et al.*, *ibid.*, p. 8045; N. Kitaguchi *et al.*, *Biochim. Biophys. Acta.* **1038**, 105 (1990); E. H. Koo *et al.*, *Proc. Natl. Acad. Sci. U.S.A.* **87**, 1561 (1990); S. S. Sisodia, E. H. Koo, K. Beyreuther, A. Unterbeck, D. L. Price, *Science* **248**, 492 (1990); W. E. Van Nostrand, A. H. Schmaier, J. S. Farrow, D. D. Cunningham, *ibid.*, p. 745; F. S. Esch *et al.*, *ibid.*, p. 1122; R. P. Smith, D. A. Higuchi, G. J. Broze, Jr., *ibid.*, p. 1126.
7. M. Hollosi, L. Otuos, Jr., J. Kajtar, A. Percel, V. M.-Y. Lee, *Pept. Res.* **2**, 109 (1989).
8. K. Halverson, P. E. Fraser, D. A. Kirschner, P. T. Lansbury, Jr., *Biochemistry* **29**, 2639 (1990).
9. E. D. Eanes, G. G. Glenner, *J. Histochem. Cytochem.* **16**, 673 (1968); D. A. Kirschner, C. Abraham, D. J. Selkoe, *Proc. Natl. Acad. Sci. U.S.A.* **83**, 503 (1986).
10. D. A. Kirschner *et al.*, *Proc. Natl. Acad. Sci. U.S.A.* **84**, 6953 (1987); P. D. Gorevic, E. M. Castano, R. Sarma, B. Frangione, *Biochem. Biophys. Res. Commun.* **147**, 854 (1987).
11. N. Greenfield and G. D. Fasman, *Biochemistry* **8**, 4108 (1969).
12. C. T. Chang, C.-S. C. Wu, J. T. Yang, *Anal. Biochem.* **91**, 13 (1978).
13. J. W. Nelson and N. R. Kallenbach, *Proteins* **1**, 211

(1986); *Biochemistry* **28**, 5256 (1989).
14. J. J. Osterhout *et al.*, *Biochemistry* **28**, 7059 (1989).
15. K. Wuthrich, *NMR of Proteins and Nucleic Acids*, (Wiley, New York, 1986); A. Bax, *Annu. Rev. Biochem.* **58**, 223 (1989); A. M. Gronenborn and G. M. Clore, *Anal. Chem.* **62**, 2 (1990).
16. P. N. Lewis, F. A. Momany, H. A. Scheraga, *Proc. Natl. Acad. Sci. U.S.A.* **68**, 2293 (1971).
17. G. E. Schulz and R. H. Schirmer, *Principles of Protein Structure* (Springer-Verlag, New York, 1979), p. 75.
18. M. G. Spillantini, M. Goldert, R. Jakes, A. Klug, *Proc. Natl. Acad. Sci. U.S.A.* **87**, 3947 (1990).
19. F. Prelli, E. Castano, G. G. Glenner, B. Frangione, *J. Neurochem.* **51**, 648 (1988).
20. H. Yamaguchi, S. Hirai, M. Morimatsu, M. Shoji, Y. Harigaya, *Acta Neuropathol.* **77**, 113 (1988); F. Tagliavini, G. Giaccone, B. Frangione, O. Bugiani, *Neurosci. Lett.* **93**, 191 (1988).
21. J. M. Candy *et al.*, *Lancet* **i**, 354 (1986); N. Behrouz, A. Defossez, A. Delacourte, P. Hublau, M. Mazzuca, *Lab. Invest.* **61**, 576 (1989).
22. D. D. Gilboe, D. B. Kinter, S. E. Emoto, J. H. Fitzpatrick, Jr., in *Pharmacology of Cerebral Ischemia*, J. Krieglstein, Ed. (Elsevier, New York, 1986), pp. 119–130; K. Munckata and K. A. Hossmann, *Stroke* **18**, 412 (1987).
23. A. M. Cataldo and R. A. Nixon, *Proc. Natl. Acad. Sci. U.S.A.* **87**, 3861 (1990).
24. C. M. Yates, J. Butterworth, M. C. Tennant, and A. Gordon [*J. Neurochem.* **55**, 1624 (1990)] have shown that brains from patients who die after AD are more acidic (because of higher lactate concentrations) than brains from patients who die suddenly with no brain disease.
25. Abbreviations for the amino acid residues are A, Ala; D, Asp; E, Glu; F, Phe; G, Gly, H, His; I, Ile; K, Lys; L, Leu; M, Met; N, Asn; Q, Gln; R, Arg; S, Ser; T, Thr; V, Val; and Y, Tyr.
26. J. M. Stewart and J. D. Young, *Solid Phase Peptide Synthesis* (Pierce Chemical, Rockford, IL, 1984).
27. We thank P. Kenny and C. Costello for mass spectroscopic analysis and K. Nakanishi, Y. Lin, and Y. Horikawa for helpful discussions.

11 December 1990; accepted 19 March 1991

Novel Enzymic Hydrolytic Dehalogenation of a Chlorinated Aromatic

JEFFREY D. SCHOLTEN, KAI-HSUAN CHANG, PATRICIA C. BABBITT, HUGUES CHAREST, MICHEL SYLVESTRE, DEBRA DUNAWAY-MARIANO*

Microbial enzyme systems may be used in the biodegradation of persistent environmental pollutants. The three polypeptide components of one such system, the 4-chlorobenzoate dehalogenase system, have been isolated, and the chemical steps of the 4-hydroxybenzoate–forming reaction that they catalyze have been identified. The genes contained within a 4.5-kilobase *Pseudomonas* sp. strain CBS3 chromosomal DNA fragment that encode dehalogenase activity were selectively expressed in transformed *Escherichia coli*. Oligonucleotide sequencing revealed a stretch of homology between the 57-kilodalton (kD) polypeptide and several magnesium adenosine triphosphate (MgATP)–cleaving enzymes that allowed MgATP and coenzyme A (CoA) to be identified as the dehalogenase cosubstrate and cofactor, respectively. The dehalogenase activity arises from two components, a 4-chlorobenzoate:CoA ligase–dehalogenase (an αβ dimer of the 57- and 30-kD polypeptides) and a thioesterase (the 16-kD polypeptide).

CHLOROAROMATICS RANK AMONG the most prevalent and environmentally persistent class of synthetic chemicals. Because standard methodologies have proved ineffective in removing these pollutants from the environment, other strategies are evolving. One strategy involves the isolation of microbes that, through a catabolic process, can transform these compounds to harmless end products. Microbial biodegradation of chloroaromatics (*1*) is, however, complicated in that the chlorine atoms interfere with the enzymatic breakdown of the aromatic ring. Some strains of bacteria have overcome this problem by incorporating a dehalogenation step at the start of the catabolic pathway.

Studies have shown that 4-chlorobenzoate (4-CBA) dehalogenase activity exists in *Pseudomonas* sp. strain CBS3 (*2*), *Nocardia* sp. (*3*), *Alcaligenes* sp. *NTP-1* (*4*), and *Arthrobacter* sp. (*5*). These bacteria were isolated from soil based on their ability to survive on 4-CBA as a sole carbon source. In each of these microbes, 4-CBA is first converted to 4-hydroxybenzoate (4-HBA), which in turn is degraded by the enzymes of the protocatechuate branch of the β-keto-adipate pathway. Substrates labeled with ^{18}O, in conjunction with crude protein powders, were used to demonstrate that in *Pseudomonas* sp. strain CBS3 (*6*) and *Arthrobacter* sp. (*7*) the conversion of 4-CBA to 4-HBA occurs by a hydrolytic process (Eq. 1), as opposed to an oxidative one. This observation suggested to us that the 4-CBA dehalogenase of these strains catalyzes a novel aromatic substitution reaction, one that conceivably might be expanded, through active site modification, to other halogenated aromatic substrates. We report the purification and characterization of an enzyme capable of catalyzing hydrolytic dechlorination of chlorinated aromatics.

Earlier attempts to purify active 4-CBA

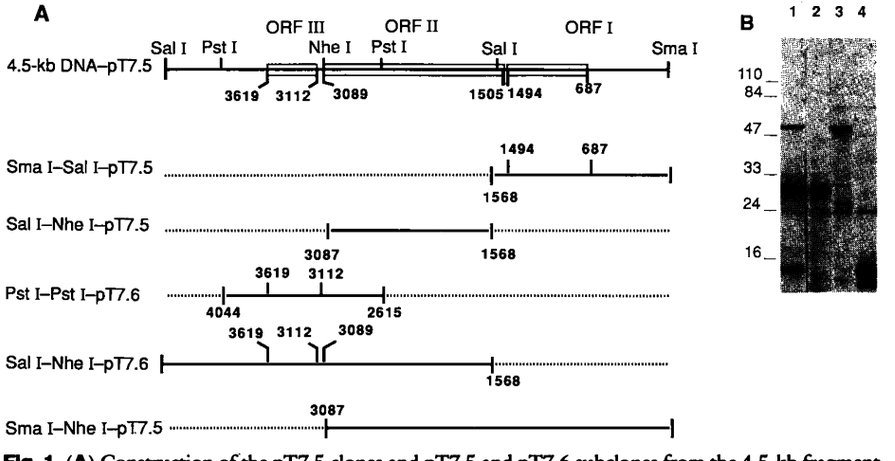

Fig. 1. (**A**) Construction of the pT7.5 clones and pT7.5 and pT7.6 subclones from the 4.5-kb fragment encoding the 4-CBA dehalogenase derived from the chromosomal DNA of *Pseudomonas* sp. strain CBS3. We generated the subclones by, and named them according to, the restriction enzymes indicated. The positions of the open reading frames ORF I, ORF II, and ORF III (identified with oligonucleotide sequencing) that encode the 30-, 57-, and 16-kD polypeptides are shown. (**B**) The autoradiogram of a 12% SDS-PAGE chromatogram of soluble cellular proteins produced by the *E. coli* k38 treated with [^{35}S]Met. Lanes are as follows: pGP1-2 and the 4.5-kb DNA-pT7.5 (lane 1), the Sma I–Sal I–pT7.5 digest (lane 2), the Sal I–Nhe I–pT7.5 digest (lane 3), or the Pst I–Pst I–pT7.6 digest (lane 4). The running positions of commercial stained molecular mass markers are indicated at left in kilodaltons.

J. D. Scholten, K.-H. Chang, D. Dunaway-Mariano, Department of Chemistry and Biochemistry, University of Maryland, College Park, MD 20742.
P. C. Babbitt, Department of Pharmaceutical Chemistry, University of California, San Francisco, CA 94145.
H. Charest and M. Sylvestre, Universite du Quebec, Institut National de la Recherche Scientifique–Santé, Pointe-Claire, Quebec, Canada H9R 1G6.

*To whom correspondence should be addressed.